Hong Kong J Radiol. 2017;20:17-27 | DOI: 10.12809/hkjr1716848

REVIEW ARTICLE

Magnetic Resonance Imaging of Ligamentous Injuries in Ankle Sprain

PY Chu, WSW Chan, HC Lee, YW Hon, JCS Chan, KKL Lo

Department of Radiology and Organ Imaging, United Christian Hospital, Kwun Tong, Hong Kong

ABSTRACT

Ankle sprains are common. Injury to the ankle ligaments is increasingly diagnosed by magnetic resonance imaging (MRI). In this review, 3-dimensional MRI sequence is discussed, the normal and injured MRI appearance of various components of the ankle ligaments is illustrated, and associated complications of ankle sprain are briefly presented.

Key Words: *Ankle injuries; Ligament; Magnetic resonance imaging*

中文摘要

踝關節韌帶扭傷的磁共振成像

朱炳容、陳施媛、李匡正、韓予偉、陳志生、勞結蓮

踝關節扭傷是一種常見的受傷。磁共振成像（MRI）技術越來越多地被應用於踝關節受傷的診斷。在本綜述中，我們討論了三維MRI序列，正常和損傷後各種踝關節韌帶的MRI表現，及踝關節扭傷的相關併發症。

INTRODUCTION

Ligamentous injury caused by excessive range of motion at the joint in the absence of fracture or dislocation is called a sprain. Ankle sprain is common and accounts for >90% of ankle injuries sustained in football, hockey, basketball, martial arts, and indoor volleyball.[1] Subsequent re-injury can result in chronic instability and disability.[2] Treatment of acute ligament injuries is based on clinical history and physical examination. With its multiplanar capability and superb soft tissue contrast, magnetic resonance imaging (MRI) is the tool of choice to evaluate the extent of ligament injuries in ankle sprain.[3] MRI helps differentiate ligament injuries from other causes of ankle pain such as fracture, osteochondral injury, and tendon injury.

We review the MRI technique for the ankle, describe the normal and injured MRI features of various components of the ankle ligaments, the associated complication of sinus tarsi syndrome, and discuss the management of ligament injuries.

IMAGING TECHNIQUE

In our institution, routine MRI of the ankle is performed

Correspondence: *Dr PY Chu, Department of Radiology and Organ Imaging, United Christian Hospital, 130 Hip Wo Street, Kwun Tong, Hong Kong.*
Email: idleadam@hotmail.com

Submitted: 17 Jan 2017; Accepted: 6 Feb 2017.

Disclosure of Conflicts of Interest: All authors have disclosed no conflicts of interest.

by experienced radiologists using a 1.5-T magnetic resonance scanner (MAGNETOM Aera; Siemens Medical Solutions, Erlangen, Germany). Axial, coronal, and sagittal planes are obtained. The ankle is imaged in the oblique axial plane parallel to the talar dome, the oblique coronal plane perpendicular to the long axis of the calcaneus, and the oblique sagittal plane parallel to bilateral malleoli and perpendicular to the talar dome. The patient is positioned supine with the foot in slight plantar flexion. Plantar flexion can decrease the magic angle effect, accentuate the fat plane between the peroneal tendons, and better visualise the calcaneofibular ligament (CFL).[4] A dedicated extremity surface coil (Foot/Ankle 16-Channel Coil; Siemens Medical Solution) is used to enhance spatial resolution. The standard MRI protocol for evaluation of ankle ligamentous injury is summarised in the Table.

Three-dimensional Magnetic Resonance Imaging Pulse Sequences

Three-dimensional (3D) MRI sequences have the advantage of acquiring thin continuous slices that reduce the effects of partial volume averaging.[5] 3D MRI sequences with isotropic resolution enable high-quality multiplanar reformat images to be obtained following a single acquisition.[5] Preliminary results for the diagnostic performance of 3D isotropic resolution sequences are encouraging. 3D MRI sequences have been reported to have 94% accuracy in detecting anterior talofibular ligament (ATFL) and CFL tears, and 92% sensitivity and 100% specificity in diagnosing ATFL and CFL rupture.[6]

A variety of 3D MRI pulse sequences have been used to detect internal derangement of joints. These include gradient-echo and fast spin-echo (FSE) 3D acquisition sequences.[7] Potential disadvantages of gradient-echo 3D MRI techniques include the relatively long acquisition time and inherent sensitivity to intravoxel dephasing and susceptibility artefacts.[7] FSE 3D pulse sequences use parallel imaging, long-echo trains, and large turbo factors to reduce imaging time.[8] The contrast characteristics in FSE 3D pulse sequence images are similar to those of FSE sequences and are a more attractive option than gradient-echo 3D pulse sequences.[7] Such 3D FSE pulse sequences include sampling perfection with application-optimised contrasts with different flip-angle evolutions (SPACE) by Siemens Healthcare[9] and extended echo-train acquisition and FSE-Cube acquisition by GE Healthcare.[10,11]

At our institution, 3D MRI pulse sequences are incorporated into ankle MRI protocols. We use FSE proton density (PD)-weighted 3D pulse sequence SPACE. It is particularly important in the evaluation of ankle ligaments as they are often obliquely oriented to the standard anatomic orthogonal imaging planes. 3D isotropic pulse sequences enable generation of multiple high-quality post-processing reformatted images from an original isotropic data acquisition along any user-defined imaging plane (Figure 1) using picture archiving and communication system station (IMPAX; Agfa Healthcare, NV, Belgium).

ANATOMY OF ANKLE LIGAMENTS

The ankle joint is supported by three groups of ligaments: lateral collateral ligaments, medial collateral ligaments, and the syndesmotic ligament complex. Ligaments that generally appear homogeneously hypointense on all imaging sequences may include the ATFL, CFL, and superficial deltoid ligament.[12] Other ankle ligaments may show a mixed or striated signal intensity pattern; these include the posterior talofibular ligament (PTFL), posterior tibiofibular ligament, and deep deltoid ligament.[4] Nonetheless, there are exceptions to typical appearances. Awareness of the normal and atypical MRI characteristics of ankle ligaments may improve diagnostic accuracy.

Table. Routine magnetic resonance imaging protocols for the ankle.

Sequence	FOV (mm)	TR (ms)	TE (ms)	Matrix	Slice thickness (mm)
Axial PDW TSE, FS	150	3500	31	256 x 256	3
Axial T2-weighted TSE, FS	150	4190	77	256 x 256	3
Coronal PDW TSE, FS	160	3500	36	162 x 320	3
Sagittal T1-weighted, no FS	150	400	11	240 x 320	3
Sagittal T2-weighted TSE, FS	150	3000	73	256 x 256	3
Coronal 3D PDW SPACE TSE, no FS	23	1100	23	156 x 256	0.6

Abbreviations: 3D = 3-dimensional; FOV = field of view; FS = fat saturation; PDW = proton density-weighted; SPACE = sampling perfection with application-optimised contrast with different flip-angle evolutions; TE = echo time; TR = repetition time; TSE = turbo spin-echo.

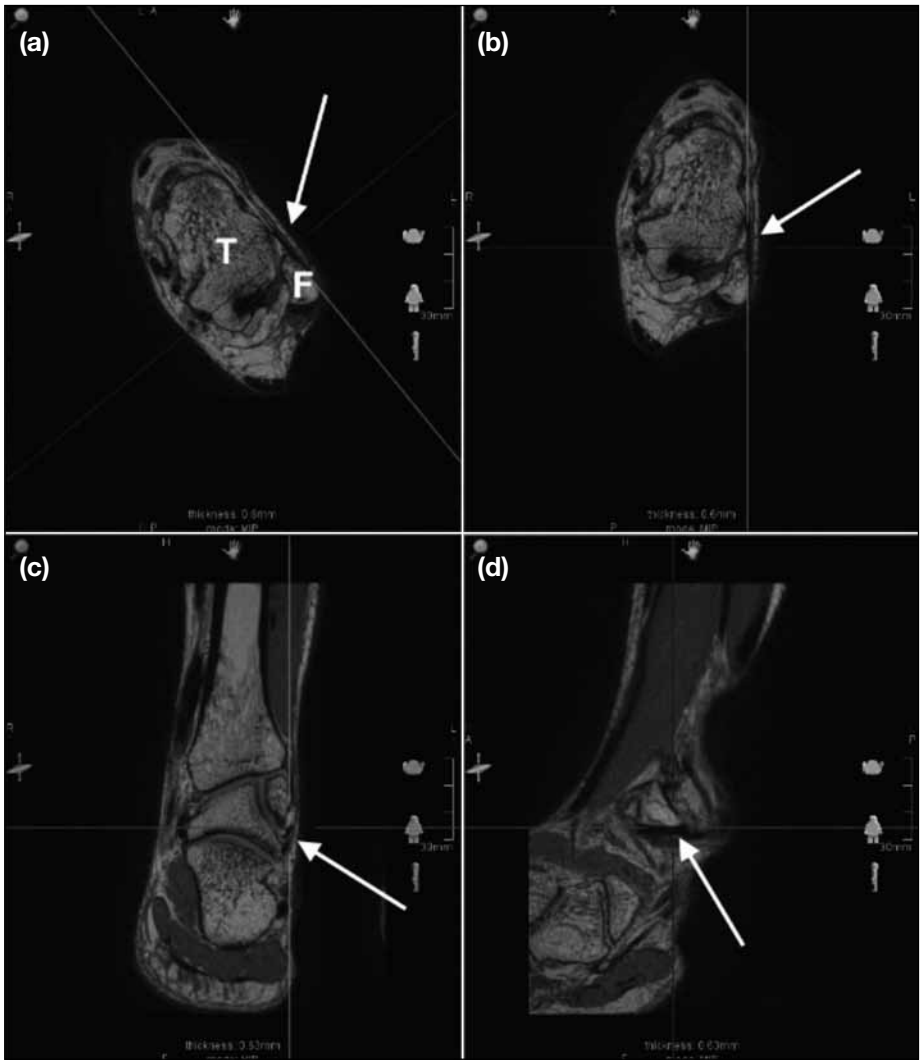

Figure 1. (a) to (d) Normal anterior talofibular ligament (ATFL) on fast spin-echo proton density–weighted three-dimensional SPACE image: the ATFL (arrows) extends from the anterior aspect of the tip of lateral malleolus of the fibula (F) and courses anteromedially downward to the talar neck (T). It is thin, straight, and of low signal intensity.
Abbreviation: SPACE = sampling perfection with application-optimised contrasts using different flip angle evolutions.

The lateral collateral ligament complex includes the ATFL, PTFL, and CFL. The ATFL extends from the anterior aspect of the lateral malleolus and courses anteromedially downward to attach onto the talar neck (Figure 2). It is best demonstrated on axial T1-wighted or high-resolution PD-weighted MRI. It usually appears as a thin, flat, and straight low-signal-intensity band in a single axial image. In most cases, ATFL actually consists of two separate fascicles, and occasionally of one or more fascicles.[13,14] The fascicles may not be differentiated in the axial plane, although may be depicted with high-resolution images (Figure 2).[14] The ATFL may also appear striated with mildly increased intra-ligamentous signal intensity on T2-weighted and PD-weighted images.[15]

The PTFL has a broad, fan-shaped appearance extending from the fibular fossa of the distal fibula, running horizontally and attaching to the posterior talar process (Figure 2). It is the strongest component of the lateral collateral ligament complex. It is best demonstrated on axial and coronal images, appearing striated due to the presence of interspersed fat. It often has marked heterogeneity and thickening, with high-signal elements on fat-suppressed sequences, which is normal and should not be interpreted as a tear.[4] The PTFL and the posterior intermalleolar ligament course transversely behind the tibiotalar joint and are typically seen as punctate low-signal-intensity structures posteriorly in the sagittal plane, potentially mimicking intraarticular bodies in the posterior ankle.[16] It is important to track each of these ligaments from their origin to their insertion on orthogonal imaging planes to avoid misdiagnosis. In addition, the pseudodefect of the

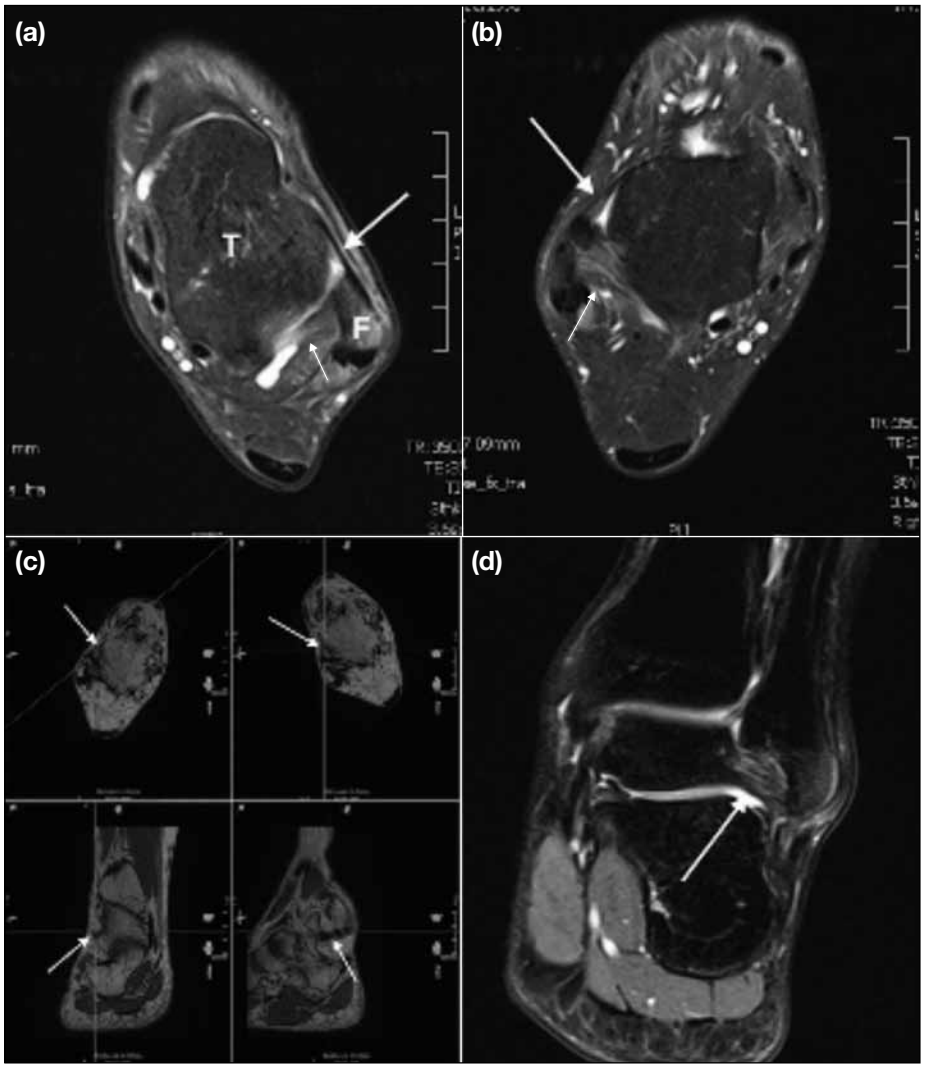

Figure 2. Normal anterior and posterior talofibular ligament (ATFL and PTFL): (a) axial proton density (PD)-weighted image with fat saturation showing ATFL (arrow) as a straight, thin, low-signal-intensity band between the tip of fibula (F) and talus (T). The talus (T) is oblong-shaped and the medial indentation of the fibula (F) represents the malleolar fossa. The PTFL (thin arrow) showing a broad, fan-shaped appearance with striated pattern due to interspersed fat. It extends from the posterior talus (T) to the fibular malleolar fossa (F). (b) In another patient, the ATFL is shown as two separate fascicles with interspersed intermediate signal intensity (arrow). The PTFL (thin arrow) is also shown. (c) Reformatted turbo spin-echo PD-weighted 3D SPACE images better demonstrate the thin linear fascicles of the ATFL (arrows). (d) Coronal T2-weighted image with fat saturation showing normal striated pattern of the PTFL (arrow).
Abbreviation: SPACE = sampling perfection with application-optimised contrasts using different flip angle evolutions.

talus represents a normal groove containing the PTFL.[17]

The ATFL and PTFL can be distinguished from the anterior and posterior inferior tibiofibular ligament (AiTFL and PiTFL) by the morphological appearance of the talus and the distal fibula on axial MRI.[18] The ATFL and PTFL are located inferior to the AiTFL and PiTFL, respectively, where the talus is oblong and the fibula demonstrates a medial indentation representing the malleolar fossa (Figures 1 and 2). AiTFL and PiTFL are detected in the talar dome that is somewhat square. In addition, these ligaments insert onto the fibula above the malleolar fossa, where the fibula is round with a flat medial border.

The CFL extends from the tip of the lateral malleolus posteroinferiorly to attach to a small tubercle on the lateral aspect of the calcaneus. It is best demonstrated on coronal and axial images. It appears as a thin low-signal-intensity band deep to the peroneal tendons and is often incompletely visualised due to its oblique orientation (Figure 3).[12] The complete course of the CFL can usually be depicted using multiplanar reconstruction from thin-section 3D MRI sequences (Figure 3).

The medial collateral ligament complex, also known as the deltoid ligament, consists of deep and superficial layers (Figure 4). The deep ligaments have talar attachment and cross one joint, and consist of anterior and posterior tibiotalar ligaments. The superficial ligaments have variable attachments and cross two joints. The three components of the superficial layer are

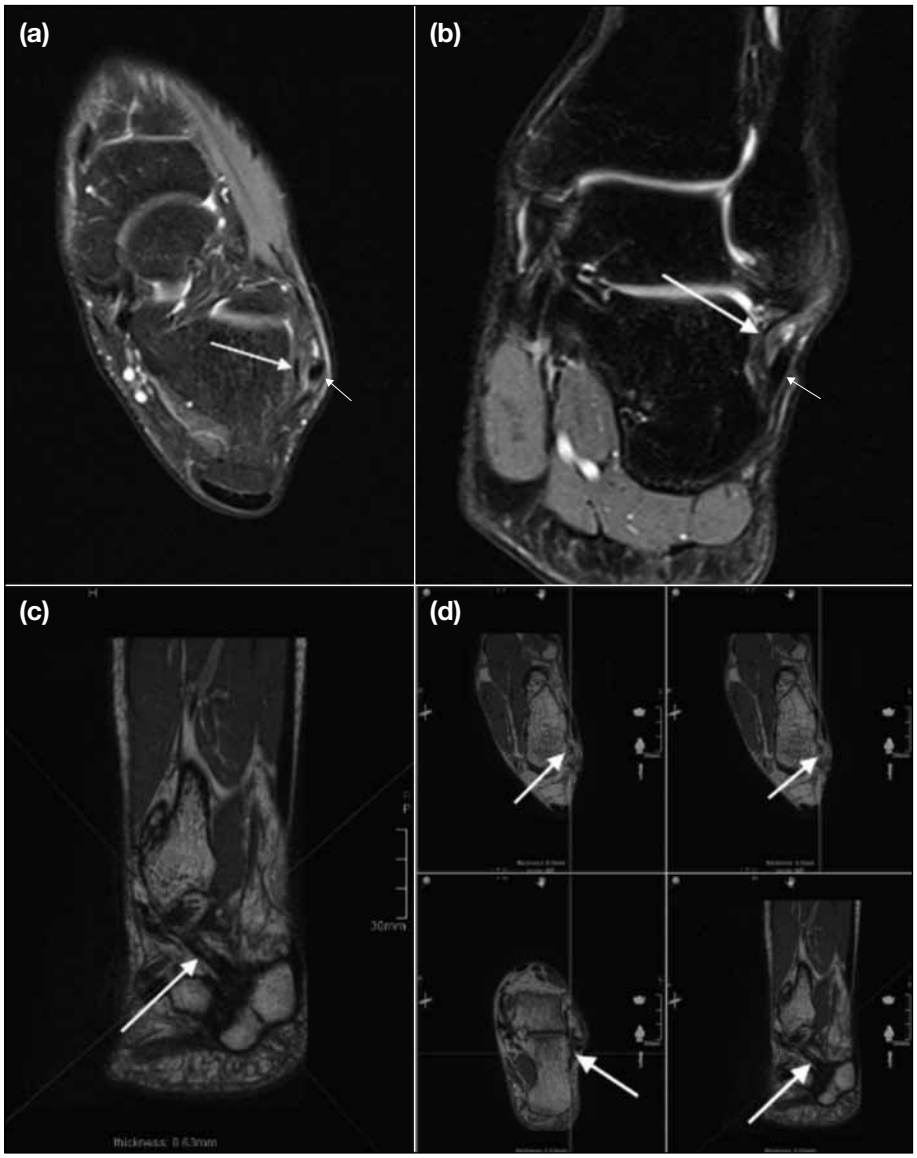

Figure 3. Normal calcaneofibular ligament: (a) axial proton density (PD)-weighted image with fat saturation showing the calcaneofibular ligament (arrow) as a thin low-signal-intensity band deep to the peroneal tendons (thin arrow) and is incompletely visualised due to its oblique orientation. (b) Coronal T2-weighted image with fat saturation showing the calcaneofibular ligament (arrow) as a thin low-signal-intensity band deep to the peroneal tendons (thin arrow) and is also incompletely visualised. Multiple images are often needed to visualise the entire course of the calcaneofibular ligament. (c) Sagittal turbo spin-echo PD-weighted 3D SPACE image showing the course of the calcaneofibular ligament (arrow) from the tip of the lateral malleolus to the small tubercle on the lateral aspect of the calcaneus. (d) Reformatted SPACE images showing the entire course of the calcaneaofibular ligament (arrows).
Abbreviation: SPACE = sampling perfection with application-optimised contrasts using different flip angle evolutions.

the tibiocalcaneal ligament, tibionavicular ligament, and tibiospring ligament. These components are variably present.[19] On standard MRI, the tibionavicular ligament and anterior tibiotalar ligament may not always be visible.[20] The mostly present components include the tibiocalcaneal ligament and tibiospring ligament in the superficial layer, and the posterior tibiotalar ligament in the deep layer.[20] The various components of the deltoid ligament are usually best demonstrated on axial and coronal images. The posterior tibiotalar component is the strongest and the most readily visualised component. It extends between the tip of the medial malleolus to the medial talar surface. It is a thick structure comprising multiple fascicles and has a striated appearance due to the presence of intervening fat between its fibres. It should not be confused with injury.[19]

The syndesmotic ligaments consist of the AiTFL, PiTFL, inferior transverse tibiofibular ligament, and inferior interosseous ligament or membrane. These ligaments are best demonstrated on axial and coronal MRI with low-to-intermediate signal intensity.[4] The AiTFL and PiTFL are usually seen on two or more sequential axial and coronal MR images at the level of the tibial plafond and talar dome (Figure 5). The AiTFL is the weakest and the most commonly torn syndesmotic ligament.[21] The AiTFL often appears striated and discontinuous due to interposition of fat between

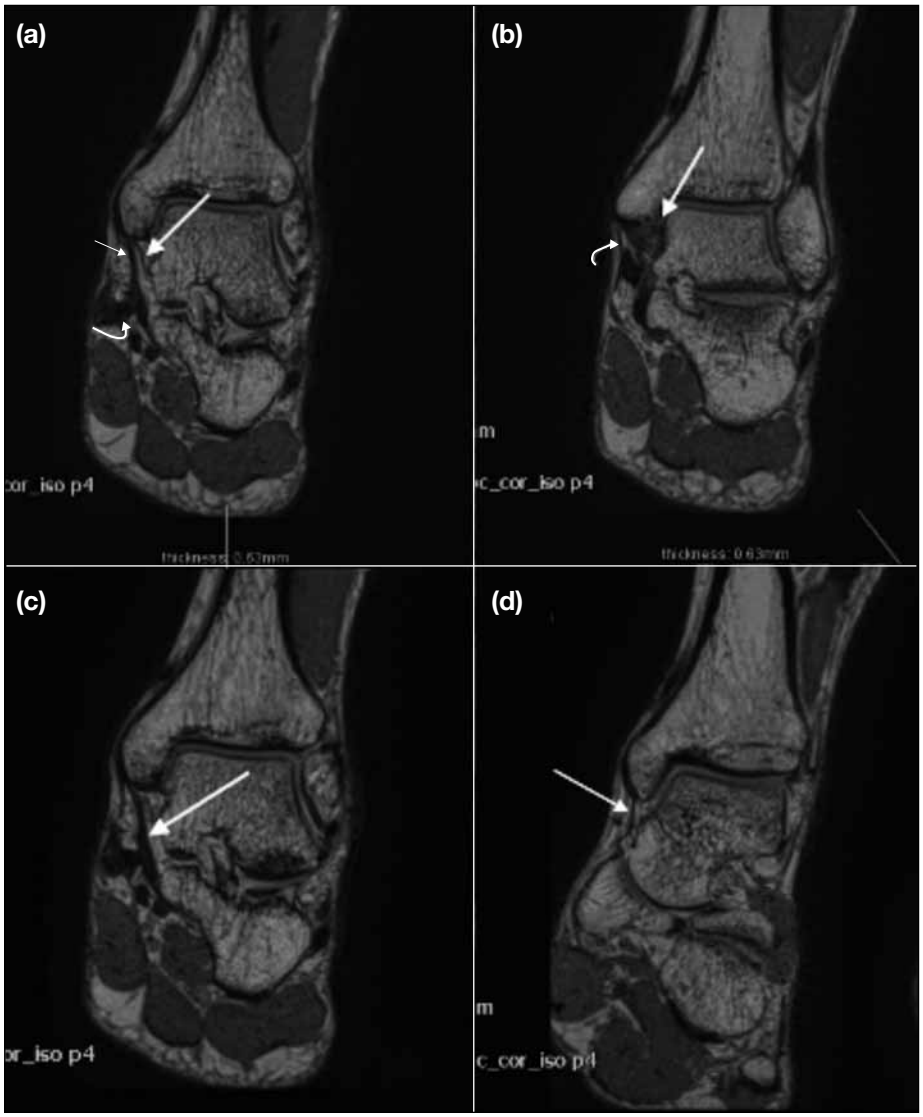

Figure 4. Normal deltoid ligament: (a) coronal turbo spin-echo proton density-weighted 3D SPACE image showing a normal anterior tibiotalar ligament (arrow), tibiospring ligament (thin arrow), and tibialis posterior tendon (curved arrow). Coronal SPACE images showing (b) a normal posterior tibiotalar ligament (arrow), with a striated appearance, and the flexor retinaculum (curved arrow), (c) a normal tibiocalcaneal ligament (arrow), and (d) a normal tibionavicular ligament (arrow).
Abbreviation: SPACE = sampling perfection with application-optimised contrasts using different flip angle evolutions.

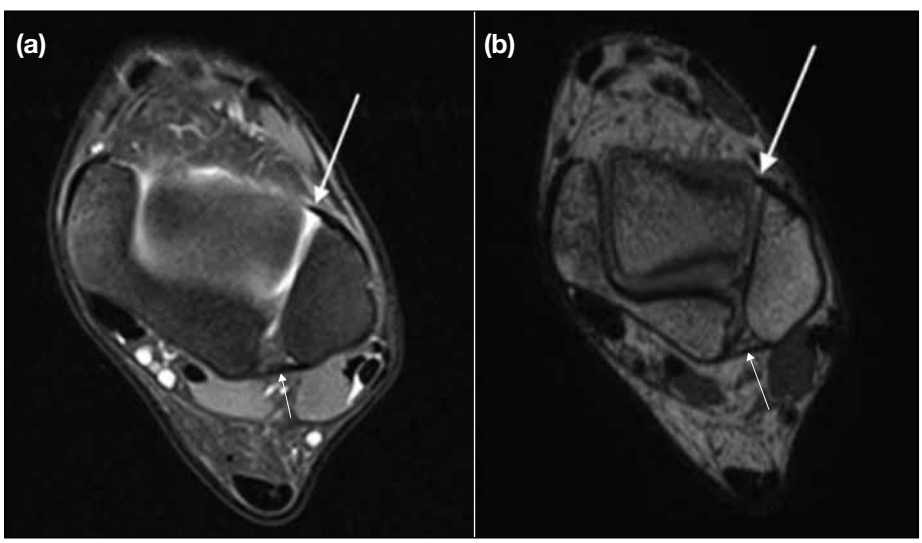

Figure 5. Normal syndesmotic ligaments: (a) axial proton density (PD)-weighted image with fat saturation showing the anterior inferior tibiofibular ligament (AiTFL) (arrow) and posterior inferior tibiofibular ligament (PiTFL) (thin arrow). (b) Axial turbo spin-echo PD-weighted 3D SPACE image showing the normal AiTFL (arrow) and PiTFL (thin arrow) as low-signal-intensity bands. They are detected in the talar dome, which is somewhat square. They insert onto the fibula above the malleolar fossa, where the fibula is oval with a flat medial border.
Abbreviation: SPACE = sampling perfection with application-optimised contrasts using different flip angle evolutions.

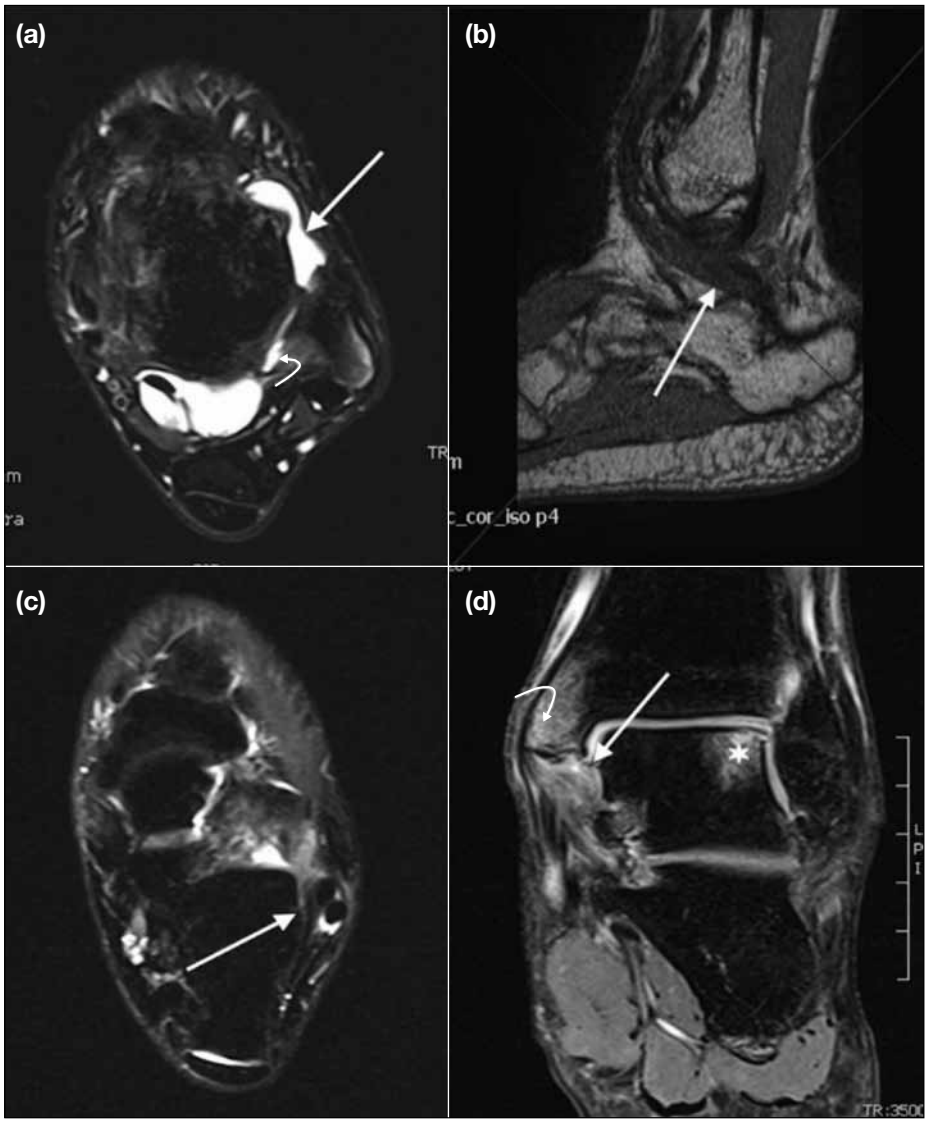

Figure 6. Acute left ankle sprain with inversion type injury in a 28-year-old man: (a) axial T2-weighted image with fat saturation showing complete absence of the anterior talofibular ligament (arrow). Partial tear of the posterior talofibular ligament at the talar attachment is also noted (curved arrow). Note the fluid at the anterolateral recess, ankle joint effusion, and fluid around the flexor hallucis longus tendon. (b) Sagittal turbo spin-echo proton density (PD)-weighted 3D SPACE showing thickened calcaneofibular ligament with intermediate signal intensity (arrow). (c) Axial T2-weighted image with fat saturation showing partial tearing of the calcaneofibular ligament (arrow). (d) Coronal PD-weighted image with fat saturation showing partial tear of the deep and superficial components of the deltoid ligament (arrow), associated bone marrow oedema (curved arrow) at the medial malleolus, and osteochondral defect at the talar dome (asterisk).
Abbreviation: SPACE = sampling perfection with application-optimised contrasts using different flip angle evolutions.

fascicles and the downward oblique course of the ligaments from the anterior tubercle of the distal tibia to the anterior tubercle of the distal fibula. It can result in depiction of a partly interrupted ligament, leading to a false-positive diagnosis of a rupture.[16]

ANKLE LIGAMENTOUS INJURIES

The MRI characteristics of acute injuries to the ankle ligaments include morphological and signal intensity alterations within and around the ligaments.[4,22] Morphological alterations may include abnormal thinning, thickening, irregularity, discontinuity, or detachment. Signal intensity alterations can be heterogeneous with increased intra-ligamentous signal intensity on fluid-sensitive MRI sequences, which indicate intra-ligamentous oedema or haemorrhage. Other associated features include obliteration of the fat planes around the ligament, extravasation of joint fluid into the adjacent spaces, and bone marrow oedema or contusion. Acute ligamentous injuries are rarely treated surgically. Concomitant injuries such as fracture, osteochondral injury, or tendon injury are common (Figures 6 to 8). These concomitant injuries are often more crucial in determining treatment and prognosis than the ligamentous injuries themselves.[4,18,19] The MRI manifestations of chronic ligamentous tear of ankle ligaments may be similar to acute injuries, which could be thickening, thinning, or irregular appearance of the

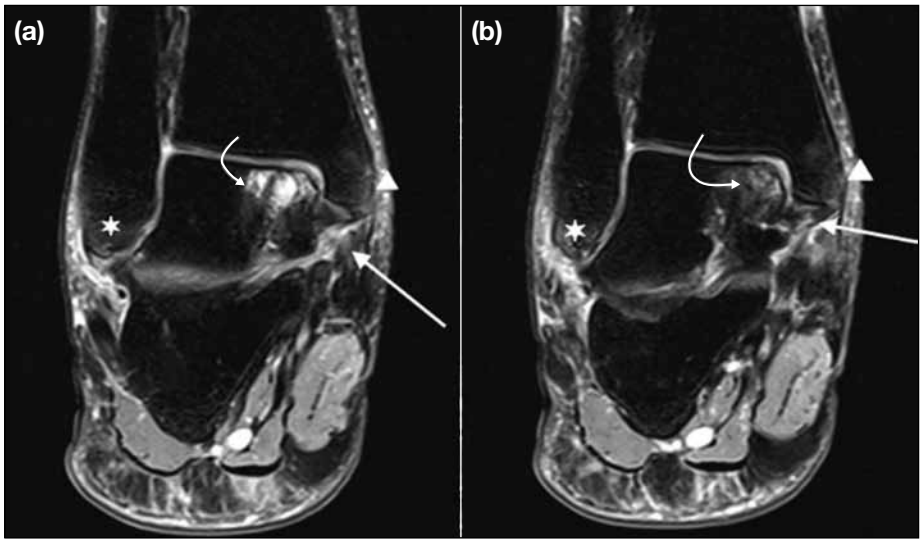

Figure 7. Subacute right ankle sprain in a middle-aged man: (a) coronal T2-weighted image with fat saturation showing full-thickness tear of the tibiospring ligament of the superficial component of the deltoid ligament (arrow). Bone marrow oedema is seen in the medial malleolus (arrowhead) with adjacent mild soft tissue swelling. There is also bone marrow oedema in the lateral malleolus (asterisk) with adjacent mild soft tissue swelling. Concomitant osteochondral injury (curved arrow) in the talar dome is seen. (b) Slightly posteriorly image showing partial tear of the deep layer of the deltoid ligament (arrow). Bone marrow oedema in the medial malleolus (arrowhead) and lateral malleolus (asterisk) with adjacent mild soft tissue swelling. Concomitant osteochondral injury (curved arrow) in the talar dome is again seen.

Figure 8. Left ankle sprain 3 months previously in a 44-year-old female: (a) plain radiography showing oblique fracture of the low shaft of the fibula suggestive of Weber type B trans-syndesmotic fracture (arrow), with no diastasis of the distal tibiofibular joint. (b) Axial proton density (PD)-weighted image with fat saturation showing complete tear of the anterior inferior tibiofibular ligament (arrow). The posterior inferior tibiofibular ligament (curved arrow) appears striated, which could be normal or due to strain / partial tear. (c) Axial PD-weighted image with fat saturation showing thickening of the anterior talofibular ligament (arrow), also evident on magnetic resonance images 2 years previously and suggestive of a chronic partial tear. (d) Coronal T2-weighted image with fat saturation showing avulsion fracture of the tip of the medial malleolus (curved arrow) and partial tear of the deep layer of the deltoid ligament (arrow).

ligaments.[4] Nonetheless, there is usually no residual soft tissue oedema or haemorrhage. Scarring or synovial proliferation may be encountered surrounding the ligaments with decreased signal intensity in all pulse sequences.

Lateral ankle sprains represent 16% to 21% of all sports-related traumatic lesions,[4] and typically occur during forced plantar flexion and inversion.[18] The ATFL is the weakest ligament and therefore the most frequently torn (Figure 6). The lateral collateral ligamentous complex usually demonstrates a predictable pattern of injury depending on the severity of ankle inversion. The ATFL is injured first, followed by the CFL and then the PTFL (Figure 6).[22] The ATFL is injured in 83% of cases, the CFL in 67%, and the PTFL in 34%.[23] Avulsion fractures of the lateral ankle ligaments are not infrequent and can be seen in up to 26% of severe inversion injuries.[24] A three-point MRI grading system is used to describe acute ankle ligament injuries.[25] Grade I injury is defined as mild sprain with superficial soft tissue oedema around the ligament. Grade II injury is a partial thickness tear and is seen as thickening / oedema and internal signal alteration within the substance of the ligament on MRI. Grade III injury is a complete tear, and MRI shows complete disruption or avulsion of the ligament. In chronic injuries of the ATFL, granulation and scar tissue may form within the anterolateral gutter, leading to impingement from entrapment of the synovial membrane between the anterior talus and the adjacent tibia or fibula.[4] This has been described as a meniscoid lesion due to its similar morphology to a meniscus in the knee. This anterolateral impingement is the most common form of ankle impingement, and patients often

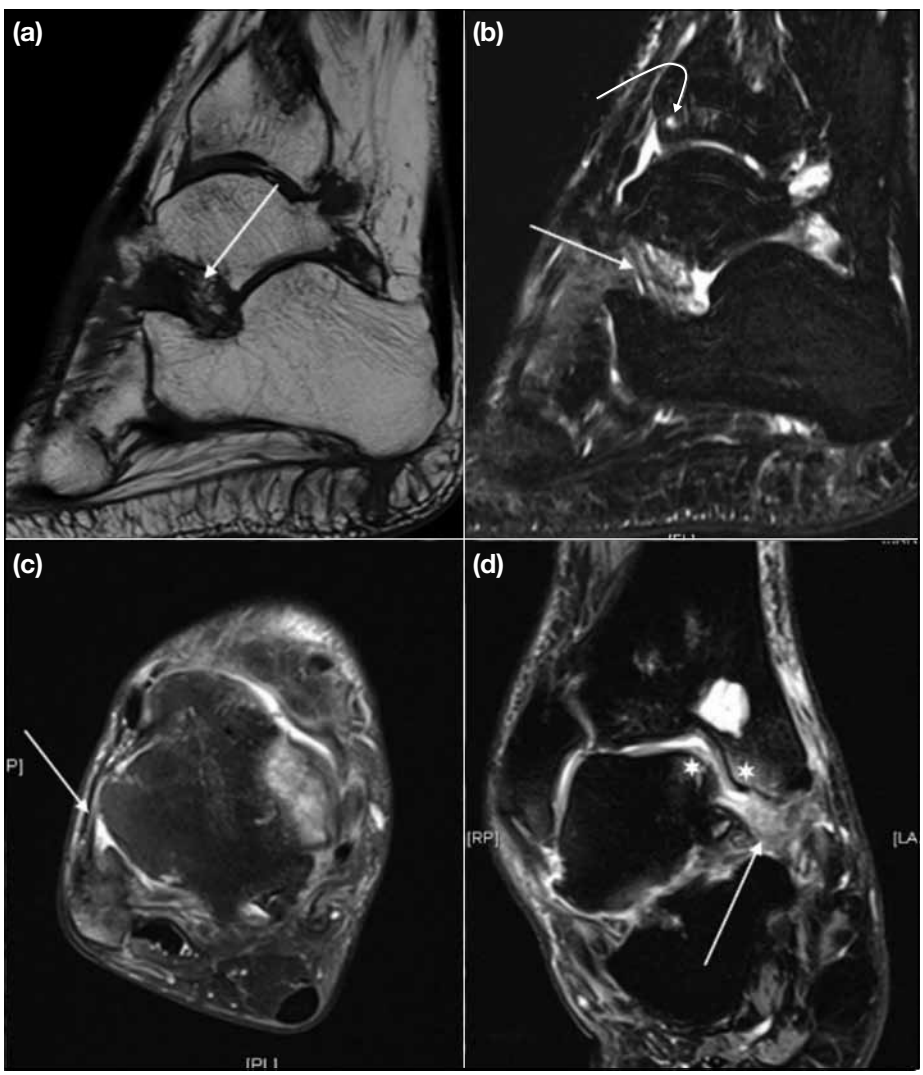

Figure 9. Right ankle pain after sprain several years ago in a 63-year-old male: (a) sagittal T1-weighted image showing loss of normal hyperintense fat signal in the sinus tarsi (arrow). (b) Sagittal T2-weighted image with fat saturation showing bright signal intensity with indistinct ligaments (arrow). A small subchondral cyst (curved arrow) is seen in the distal tibia likely due to degenerative changes. (c) Axial proton density-weighted image with fat saturation showing thin anterior talofibular ligament (arrow), likely due to prior sprain or partial tear. (d) Coronal T2-weighted image with fat saturation showing disruption of the deltoid ligament (arrow). Degenerative changes with subchondral oedema and cysts are seen (asterisks).

present with persistent lateral ankle pain and instability.

Deltoid ligament complex injuries account for about 5% of ankle sprains.[26] Pronation-eversion and extreme rotation are known to be the mechanism that leads to deltoid ligament injuries.[19] Recent studies show deltoid ligament injuries may be more frequent than previously thought.[27] Isolated deltoid ligament injuries are infrequent and often associated with lateral ligamentous injuries, syndesmotic injuries, or malleolar fractures particularly in Weber type B fracture (Figures 6 to 8).[19] The deep layer is more commonly injured than the superficial layer, and partial tears are more common than full-thickness tears.[18,19] Sprains of the deep layer of the deltoid ligament are frequently noted on MRI in patients after inversion injuries (Figure 6).[18]

Syndesmotic ligament injury or high ankle sprain accounts for approximately 7% of ankle sprains.[26] The mechanism of injury is thought to be forced external rotation with ankle dorsiflexion and pronation.[28] The AiTFL is the most commonly torn ligament, and is almost always torn before the other syndesmotic ligaments (Figure 8).[29] The injuries can be either ligamentous tear, avulsion fracture, or both. They can be isolated or may occur in conjunction with other ankle ligamentous groups, or associated with Weber B or C ankle fractures.[30] It is associated with a greater risk of chronic ankle dysfunction and persistent pain and usually requires a longer time to recover previous level of function, compared with other ankle sprains of similar severity that do not involve the syndesmosis.[31]

POST-TRAUMATIC SINUS TARSI SYNDROME

The sinus tarsi is a cone-shaped cavity in the lateral aspect of the midfoot between the anterosuperior aspect of the calcaneus and the inferior aspect of the talar neck. It opens laterally anterior to the lateral malleolus and terminates posteromedially behind the sustentaculum tali. The contents of the sinus tarsi include abundant fat surrounding vessels, nerves, and a ligamentous complex that comprises the medial, intermediate, and lateral roots of the inferior extensor retinaculum, lateral cervical ligament, and medial talocalcaneal interosseous ligament. The sinus tarsi ligaments, nerves, and vessels play an important role in the stabilisation and proprioception of the subtalar joint.[32]

Sinus tarsi syndrome is a clinical syndrome characterised by persistent lateral ankle pain and hindfoot instability.[18] It is a common complication of ankle sprains; 70% of cases have a trauma history, and 30% have miscellaneous causes such as ganglion cysts, gout or pigmented villonodular synovitis.[33] Sinus tarsi syndrome is a clinical diagnosis and should not be established solely on MRI findings alone. The sinus tarsi is best evaluated on T1- and T2-weighted sagittal images. In MRI, the normal sinus tarsi is T1-weighted hyperintense due to abundant fat, and the ligamentous structures are clearly outlined by the bright fat signal. In sinus tarsi syndrome, the T1-weighted hyperintense fat signal is replaced with a low signal on T1-weighted images due to fluid or scar tissue, and a bright signal on T2-weighed images, with disruption of or indistinct cervical and interosseous ligaments.[4,18] Associated MRI findings include osteoarthritis of the subtalar joint with subchondral oedema or cysts of the talus or calcaneus, or contrast enhancement of the hypertrophied synovium.[4,18]

TREATMENT

Non-operative management remains the gold standard for ankle sprains.[34] In acute injuries, conservative treatment in the form of RICE (rest, ice, compression, elevation) is recommended.[34,35] Functional rehabilitation (e.g. motion restoration and strengthening exercises) remains the cornerstone of conservative treatment and is preferred over immobilisation in low-grade sprains.[35] In severe ankle sprain, treatment is controversial. Several prospective level I studies have compared non-operative treatment and operative treatment for grade III sprains and shown no significant difference in outcome.[36,37] Surgical repair may be considered in patients with persistent symptoms and instability who are recalcitrant to conservative measures.[18,34]

CONCLUSION

It is important for the radiologist to recognise the complex ligamentous structures in the ankle, including the normal anatomic variants and imaging pitfalls. Better understanding of the MRI appearance of various ligamentous injuries and the associated pathological conditions may help guide clinical decision making for early and appropriate intervention, and thus prevent long-term morbidity.

REFERENCES

1. Fong DT, Hong Y, Chan LK, Yung PS, Chan KM. A systematic review on ankle injury and ankle sprain in sports. Sports Med. 2007;37:73-94. crossref
2. Marchi AG, Di Bello D, Messi G, Gazzola G. Permanent sequelae in sports injuries: a population based study. Arch Dis Child.

1999;81:324-8. cross ref
3. Aerts P, Disler DG. Abnormalities of the foot and ankle: MR imaging findings. AJR Am J Roentgenol. 1995;165:119-24. cross ref
4. Rosenberg ZS, Beltran J, Bencardino JT. From the RSNA Refresher Courses. Radiological Society of North America. MR Imaging of the ankle and foot. Radiographics. 2000;20:S153-79. cross ref
5. Kijowski R, Gold GE. Routine 3D magnetic resonance imaging of joints. J Magn Reson Imaging. 2011;33:758-71. cross ref
6. Verhaven EF, Shahabpour M, Handelberg FW, Vaes PH, Opdecam PJ. The accuracy of three-dimensional magnetic resonance imaging in the diagnosis of ruptures of the lateral ligaments of the ankle. Am J Sports Med. 1991;19:583-7. cross ref
7. Naraghi A, White LM. Three-dimensional MRI of the musculoskeletal system. AJR Am J Roentgenol. 2012;199:W283-93. cross ref
8. Park J, Mugler JP 3rd, Horger W, Kiefer B. Optimized T1-weighted contrast for single-slab 3D turbo spin-echo imaging with long echo trains: application to whole-brain imaging. Magn Reson Med. 2007;58:982-92. cross ref
9. Lichy MP, Wietek BM, Mugler JP 3rd, Horger W, Menzel MI, Anastasiadis A, et al. Magnetic resonance imaging of the body trunk using a single-slab, 3-dimensional, T2-weighted turbo-spin-echo sequence with high sampling efficiency (SPACE) for high spatial resolution imaging: initial clinical experiences. Invest Radiol 2005;40:754-60. cross ref
10. Gold GE, Busse RF, Beehler C, Han E, Brau AC, Beatty PJ, et al. Isotropic MRI of the knee with 3D fast spin-echo extended echo-train acquisition (XETA): initial experience. AJR Am J Roentgenol. 2007;188:1287-93. cross ref
11. Ristow O, Steinbach L, Sabo G, Krug R, Huber M, Rauscher I, et al. Isotropic 3D fast spin-echo imaging versus standard 2D imaging at 3.0 T of the knee: image quality and diagnostic performance. Eur Radiol. 2009;19:1263-72. cross ref
12. Muhle C, Frank LR, Rand T, Yeh L, Wong EC, Skaf A, et al. Collateral ligaments of the ankle: high-resolution MR imaging with a local gradient coil and anatomic correlation in cadavers. Radiographics. 1999;19:673-83. cross ref
13. Milner CE, Soames RW. Anatomical variations of the anterior talofibular ligament of the human ankle joint. J Anat. 1997;191:457-8. cross ref
14. Choo HJ, Lee SJ, Kim DW, Jeong HW, Gwak H. Multibanded anterior talofibular ligaments in normal ankles and sprained ankles using 3D isotropic proton density-weighted fast spin-echo MRI sequence. AJR Am J Roentgenol. 2014;202:W87-94. cross ref
15. Delfaut EM, Demondion X, Boutry N, Cotten H, Mestdagh H, Cotten A. Multi-fasciculated anterior talo-fibular ligament: reassessment of normal findings. Eur Radiol. 2003;13:1836-42. cross ref
16. Gyftopoulos S, Bencardino JT. Normal variants and pitfalls in MR imaging of the ankle and foot. Magn Reson Imaging Clin N Am. 2010;18:691-705. cross ref
17. Arnold G, Vohra S, Marcantonio D, Doshi S. Normal magnetic resonance imaging anatomy of the ankle & foot. Magn Reson Imaging Clin N Am. 2011;19:655-79. cross ref
18. Nazarenko A, Beltran LS, Bencardino JT. Imaging evaluation of traumatic ligamentous injuries of the ankle and foot. Radiol Clin North Am. 2013;51:455-78. cross ref
19. Chhabra A, Subhawong TK, Carrino JA. MR imaging of deltoid ligament pathologic findings and associated impingement syndromes. Radiographics. 2010;30:751-61. cross ref
20. Mengiardi B, Pfirrmann CW, Vienne P, Hodler J, Zanetti M. Medial collateral ligament complex of the ankle: MR appearance in asymptomatic subjects. Radiology. 2007;242:817-24. cross ref
21. Oae K, Takao M, Naito K, Uchio Y, Kono T, Ishida J, et al. Injury of the tibiofibular syndesmosis: value of MR imaging for diagnosis. Radiology. 2003;227:155-61. cross ref
22. Bencardino J, Rosenberg ZS, Delfaut E. MR imaging of sports injuries of the foot and ankle. Magn Reson Imaging Clin N Am. 1999;7:131-49.
23. Fallat L, Grimm DJ, Saracco JA. Sprained ankle syndrome: prevalence and analysis of 639 acute injuries. J Foot Ankle Surg. 1998;37:280-5. cross ref
24. Haraguchi N, Toga H, Shiba N, Kato F. Avulsion fracture of the lateral ankle ligament complex in severe inversion injury: incidence and clinical outcome. Am J Sports Med. 2007;35:1144-52. cross ref
25. Gonzalez FM, Morrison WB. Magnetic resonance imaging of sports injuries involving the ankle. Top Magn Reson Imaging. 2015;24:205-13. cross ref
26. Waterman BR, Belmont PJ Jr, Cameron KL, Svoboda SJ, Alitz CJ, Owens BD. Risk factors for syndesmotic and medial ankle sprain: role of sex, sport, and level of competition. Am J Sports Med. 2011;39:992-8. cross ref
27. Hintermann B, Knupp M, Pagenstert GI. Deltoid ligament injuries: diagnosis and management. Foot Ankle Clin. 2006;11:625-37. cross ref
28. Williams GN, Jones MH, Amendola A. Syndesmotic ankle sprains in athletes. Am J Sports Med. 2007;35:1197-207. cross ref
29. Rasmussen O. Stability of the ankle joint. Analysis of the function and traumatology of the ankle ligaments. Acta Orthop Scand Suppl. 1985;211:1-75. cross ref
30. Perrich KD, Goodwin DW, Hecht PJ, Cheung Y. Ankle ligaments on MRI: appearance of normal and injured ligaments. AJR Am J Roentgenol. 2009;193:687-95. cross ref
31. Amendola A, Williams G, Foster D. Evidence-based approach to treatment of acute traumatic syndesmosis (high ankle) sprains. Sports Med Arthrosc. 2006;14:232-6. cross ref
32. Lektrakul N, Chung CB, Lai Ym, Theodorou DJ, Yu J, Haghighi P, et al. Tarsal sinus: arthrographic, MR imaging, MR arthrographic, and pathologic findings in cadavers and retrospective study data in patients with sinus tarsi syndrome. Radiology. 2001;219:802-10. cross ref
33. Breitenseher MJ, Haller J, Kukla C, Gaebler C, Kaider A, Fleischmann D, et al. MRI of the sinus tarsi in acute ankle sprain injuries. J Comput Assist Tomogr. 1997;21:274-9. cross ref
34. Fong DT, Chan YY, Mok KM, Yung PSh, Chan KM. Understanding acute ankle ligamentous sprain injury in sports. Sports Med Arthrosc Rehabil Ther Technol. 2009;1:14. cross ref
35. Ivins D. Acute ankle sprain: an update. Am Fam Physician. 2006;74:1714-20.
36. Kerkhoffs GM, Handoll HH, de Bie R, Rowe BH, Struijs PA. Surgical versus conservative treatment for acute injuries of the lateral ligament complex of the ankle in adults. Cochrane Database Syst Rev. 2007;2:CD000380. cross ref
37. Povacz P, Unger SF, Miller WK, Tockner R, Resch H. A randomized, prospective study of operative and non-operative treatment of injuries of the fibular collateral ligaments of the ankle. J Bone Joint Surg Am. 1998;80:345-51. cross ref